Abstract

Bitumen extraction from the Athabasca oil sands involves large volumes of water known as oil sands process affected water (OSPW). OSPW contains naphthenic acids (NAs), a class of aliphatic and cyclic carboxylic acids that can be toxic and are recalcitrant to natural attenuation. A passive advanced oxidation process (P-AOP), such as solar photocatalysis (PC) with buoyant photocatalysts (BPCs, TiO_2-coated buoyant microspheres), is promising for NA treatment, through conversion to more hydrophilic forms (partial oxidation) or to CO_2 (complete mineralization), depending on the solar dose. Although BPCs exhibit strong reactivity, full NA mineralization can require impractical hydraulic retention times. Biodegradation is another promising passive approach, but biodegradation rates are ultimately inhibited by the toxicity and structural complexity of NAs. We hypothesized that biological NA removal kinetics could be enhanced through BPC pre-treatment, since partial oxidation can lower NA toxicity and improve their biodegradability. Different PC exposure durations were used to pre-treat simulated OSPW prior to a biological treatment stage (with natural microbial culture from OSPW), to understand their impacts on NA chemical speciation and biodegradation kinetics. PC pre-treatment (2 d) enabled full mineralization (to <3 mg/L COD) and >99.9% removal of acid-extractable organics (AEO) in secondary biological treatment (21 d). Mineralization was achieved earlier in the combined PC+bio treatment than by photocatalysis alone (33 d vs. >42.2 d), and microbial growth rate was accelerated 23-fold compared to the non-pre-treated water. Overall, BPCs can improve NA biodegradability to achieve mineralization through a fully passive combined treatment process, without chemical or energy inputs.

Key Words:

naphthenic acids, OSPW, photocatalysis, bioremediation, passive treatment, TiO_2

Mild Photocatalysis Removes Microbial Inhibition and Enables Effective Biological Treatment of Naphthenic Acids

Cassandra Chidiac[1], Timothy Michael Carter Leshuk[1,2], Frank Gu[1,2]
[1]Department of Chemical Engineering and Applied Chemistry, University of Toronto, 200 College Street, Toronto, M5S 3E5, Canada
[2]H2nanO, 151 Charles St W, Kitchener, N2G 1H6, Canada
Corresponding author: f.gu@utoronto.ca

Nomenclature Abbreviations

Abbreviation	Name	Unit
OSPW	Oil sands process affected water	-
NA	Naphthenic acids	-
AEO	Acid-extractable organics	mg/L
sCOD	Soluble chemical oxygen demand	mg/L
BOD	Biochemical oxygen demand	mg/L
MW	Molecular weight	g/mol
O/C	Oxygen to carbon ratio	mol oxygen/mol carbon
DBE	Double bond equivalence	-
OD	Optical density	-
LC-MS	Liquid chromatography-mass spectrometry	-
BPC	Buoyant photocatalysts	-
ATP	Adenosine Triphosphate	-
DNA	Deoxyribonucleic acid	-

1. Introduction

Bitumen extraction from the Athabasca Oil sands uses an alkaline hot water extraction process that produces a complex mixture of solids, residual bitumen, and contaminated water, known as oil sands process affected water (OSPW) [1–3]. In lieu of reserving freshwater resources, a zero-discharge policy has been imposed on OSPW, driving companies to recycle OSPW on-site for further extractions and causing over 1 billion m^3 to accumulate [2, 4]. Naphthenic acids (NAs) are OSPW's principal contaminant of concern and encompass a class of aliphatic and cyclic carboxylic acids with additional possible aromatic and heteroatom moieties [1, 2, 5, 6]. NAs' amphiphilic nature enables them to penetrate cell membranes, disrupt their properties and, in turn, cause cell death. This phenomenon causes acute and chronic toxic effects in aquatic life at concentrations >0.10 mg/L, where concentrations in OSPW have reached upwards of 120 mg/L due to NAs' recalcitrance to natural attenuation [1–3].

Buoyant photocatalysts (BPCs) are hollow glass microspheres coated with TiO_2 nanoparticle photocatalysts, enabling catalyst localization at waters' surfaces where they can be activated by solar light [7–10]. TiO_2 activation creates internal valence band holes that react with water and generate hydroxyl radicals, a potent oxidant [8]. Simultaneously, electrons are photogenerated in TiO_2 which reduce oxygen in solution and, in turn, produce superoxide anions capable of initiating ring-opening reactions [11]. These reactive oxygen species collectively cause hydrogen abstraction in NAs, thereby oxidizing them to more hydrophilic forms (partial mineralization) or to CO_2 (complete mineralization). Overall, BPCs are a promising passive treatment for OSPW since they enable simple TiO_2 recycling and have demonstrated high reactivity

on pertinent NA structures [8, 10, 11]. However, since PC treatment follows Langmuir-Hinshelwood kinetics, treatment rates exponentially diminish with decreasing NA concentrations. Due to the shear volume of OSPW to be treated, these kinetic hindrances could be detrimental to treatment time and resources if near-complete mineralization is required.

Biodegradation is another promising passive treatment technology for OSPW remediation since NAs can serve as a microbial carbon source [1], [12] – [14][1], [12] – [14]. Although microbes degrade simplistic NA structures via predominately β-oxidation routes, biodegradation of complex NA structures with higher alkyl branching and cyclicity are impeded due to steric hindrances [1, 12, 15]. Additionally, threshold concentrations for individual NA structures are required for their metabolism [14, 15]. Collectively, these limitations necessitate biological treatment be coupled with co- or pre-treatment processes [16–21]. It is therefore hypothesized combining PC and biological treatment could simultaneously alleviate their respective limitations, such as by using BPCs as a pre-treatment for biodegradation, since photocatalytic reactive oxygen species preferentially oxidize recalcitrant NAs (*i.e.,* higher cyclicity, alkyl branching, molecular weights) to more hydrophilic forms, which may improve their bio-availability and -degradability [1], [15] – [17][1], [15] – [17].

Although yet to be demonstrated in OSPW, photocatalytic pre-treatments have improved the biodegradation efficiencies for other recalcitrant organics, such as: methyl red [24], antibiotics [25, 26], ammonia [27] and chlorophenols [27]. Furthermore, the use of other advanced oxidative processes (AOP) (*e.g.,* ozone, electro-oxidation, persulfate oxidation) as pre-treatments have improved NA biodegradability, but the potential of creating toxic by-products, electrical usage, and chemical addition (*i.e.,* high operating costs) are critical limitations [15, 17, 19, 28–30]. BPC treatment may address these disadvantages since it offers a fully passive system (no chemical or electrical requirements) that rapidly eliminates OSPW toxicity. Herein BPC pre-treatment for NA biodegradation was investigated with the following objectives: (1) understand how photocatalysis pre-treatment times impacts subsequent NA biodegradation kinetics and removal; (2) evaluate the impact of photocatalytic pre-treatment on microbial activity; and (3) understand how photocatalytic pre-treatment impacts NA chemical speciation, and the microbial response to these respective chemical shifts.

2. Materials and Methods

2.1 Materials

OSPW brine components (NH_4Cl, $CaCl_2 \cdot 2H_2O$, $MgCl_2 \cdot 6H_2O$, KCl, $NaHCO_3$, NaF, NaCl, Na_2SO_4), lysis buffer components (NaCl, KCl, Na_2HPO_4, and KH_2PO_4), Bradford assay reagent, albumin from bovine serum albumin (lyophilized powder, pH 7, ≥ 98%), lysozyme from chicken egg white (lyophilized powder, protein ≥90%, ≥40,000 units/mg protein), dichloromethane (≥99.9% HPLC grade), sodium acetate anhydrous, sodium azide, 100 mM phosphate buffered solution pellets, and technical grade of naphthenic acids (NAs) were purchased from Sigma Aldrich Canada. Technical grade of NAs is comprised of carbon

numbers 6-20 and Z numbers between 0 to -4 as reported by Damasceno et al [31]. HCl (37%, ACS grade) and chemical oxygen demand (COD) vials was purchased from Supelco and Hach, respectively.

H_2O_2 (30 wt%) was purchased from Aldrich. 0.22 µm Nylon membranes and 0.7 µm Whatman Filter were purchased from Sigma-Aldrich, while 0.45 µm PTFE syringe filters were purchased from VWR Canada. Tetraethylorthosilicate (98%) and Pluronic 127 were purchased from Sigma-Aldrich; H_2SO_4 (95-98%, ACS grade) and ethanol (EtOH, ACS grade) was purchased from Fisher. Invitrogen ATP Determination Kit was purchased from ThermoFisher Scientific. BPCs were provided in-kind by H2nanO Inc., manufactured according to a scaled process with similar chemistry as described previously by Leshuk et al [8, 10].

2.2 Microbial Cultivation

Microbes were cultivated in a 1 L Erlenmeyer flask that was mixed at 100 rpm using a PTFE coated stir bar. The microbial seed was taken from an active tailings pond in the Athabasca region, from an anonymous oil sands industry partner OSPW. Specifically, 250 mL was pelleted and grown in synthetic OSPW brine (18.9 mg/L NH_4Cl; 36.7 mg/L $CaCl_2 \cdot 2H_2O$; 83.6 mg/L $MgCl_2 \cdot 6H_2O$, 28.6 mg/L KCl, 755.4 mg/L $NaHCO_3$, 6.6 mg/L NaF, 1.1 g/L NaCl, and 443.6 mg/L Na_2SO_4) and 40 mg/L of pre-oxidized NAs (COD_0 ~ 100 mg/L). The OSPW brine ionic composition was selected based on the average literature characterization of OSPW [8, 10, 32]. NAs (2.5 g/L) were pre-oxidized using 2 mM H_2O_2 under UV_C light (intensity ~ 3.5 ± 0.1 mW/cm^2) for 90 minutes, where radicals were subsequently quenched using excess $Na_2S_2O_3$. Pre-oxidized NAs were stored in an amber bottle at -20°C to mitigate premature degradation. COD was monitored weekly to ensure levels did not fall below <50 mg/L, where each subsequent dosage was supplemented with ~5 mg/L NH_4Cl and 1 mg/L PO_4^{2-} to maintain COD:N:P ratio of ~100:5:1 [33]. Additionally, optical density (OD) was measured weekly to monitor bacterial growth and was maintained between 0.04-0.05. OD was measured in triplicates using the Tecan Infinite M Plex Plate reader at 600 nm. Microbes were used once acclimatized to pre-oxidized NAs, as demonstrated by their consistent NA mineralization and growth over >5 cycles (Fig S.1).

2.3 Photocatalytic Treatment Design

BPCs were washed thrice prior to experiments and were dosed at 5 g/L, an optimized concentration previously determined, in 210 mL of simulated OSPW brine spiked with 40 mg/L NAs [32]. A concentration of 40 mg/L was selected since it is representative of characteristic OSPW industry samples [3]. Furthermore, the beakers' sides were wrapped with aluminum foil to eliminate light scattering and were sealed with UV transparent polyethylene film to mitigate evaporation. A pre-adsorption step was conducted in the dark for 1 h under a mixing rate of 300 rpm using a PTFE coated stir bar (7/8'' x 5/6''). Subsequently, the OSPW samples were placed under a solar UV simulator photocatalytic bed, with an array of UV_A fluorescent light bulbs (Philips F20T12/BL, peak emission ~350 nm). The UV dosage was maintained at 6.5 ± 0.3 mW/cm^2, where the intensity was measured with a $UV_{A/B}$ light meter (Sper Scientific, NIST certified calibration) 15 minutes after the reaction start time and after each reaction time. The corresponding UV dosages (kJ/L) and treatment times in the Athabasca oil sands for the allocated effective pre-treatment

times are presented in Table 1. Additionally, photolysis and dark-adsorption controls were conducted, where 2 d COD levels confirmed minimal NA mineralization (<12%).

Table 1. A Summary of Tested Photocatalytic Pre-Treatment Times (h) with their Corresponding UV Dosages (kJ/L) and Equivalent Days in the Athabasca Oil Sands. Error shown represent standard deviation.

Photocatalytic Pre-Treatment Time (h)	UV Dosage (kJ/L)	Equivalent Days in the Athabasca Oil Sands
1	1.09 ± 0.21	0.25 ± 0.05
4	4.94 ± 0.06	1.14 ± 0.01
8	9.65 ± 0.22	2.23 ± 0.05
24	28.75 ± 1.31	6.64 ± 0.30
48	52.79 ± 5.23	12.19 ± 1.21
168	182.50 ± 32.85	42.15 ± 8.05

2.4 Biological Treatment Design

Photocatalytically treated samples were filtered with 0.7 µm Whatman filters to remove BPCs, where a portion of the filtrate was used to measure COD. COD was measured using low range HACH test kits (Method 8000). Subsequently, each beaker was rinsed with deionized water thrice to remove residual BPCs. The filtrate was added into the rinsed beakers and dosed with 0.01 vol/vol of inoculum prepared as described in *Section 2.3*. Biological samples were subsequently operated under batch conditions with a mixing speed of 200 rpm with a PTFE coated stir bar (7/8'' x 5/6'') under different treatment times. An additional biosorption control was created by adding 0.04 w/v% of sodium azide to the raw sample. Once the respective biological times elapsed, the biologically treated samples were centrifuged at 5300 rpm for 90 minutes using the Avanti J-E centrifuge (Beckman Coulter) to pellet the accumulated biological masses. Cell pellets were re-suspended in 1 mL of cell lysis buffer (140 mM NaCl, 10 mM Na_2HPO_4, 7 mM KCl, 8 mM KH_2PO_4 dissolved in 10 mM PBS), and were dosed with 25 µL of lysozyme and incubated on ice for 30 minutes. Cells were lysed on ice using a sonication probe, where 3 cycles of 10 s on and 30 s off at an amplitude of 40% was used. Cell suspensions were then stored at -20°C until further analyses (*Section 2.7)*.

2.5 Microbial Inhibition Test Design

Microbial inhibition tests were conducted using 30 mL of the filtered photocatalytically treated water, where controls with untreated OSPW and OSPW brine without NAs were additionally analyzed. Each sample was dosed with 1 g/L of acetate and 1 vol/vol of inoculum. OD and sCOD (soluble chemical oxygen demand) were measured periodically to monitor microbial growth and organic removal under the different tested conditions, respectively. sCOD levels were assessed subsequently after filtering through a 0.45 µm PTFE syringe filter using high range HACH test kits (Method 8000).

2.6 Microbial ATP, Protein, and DNA Quantification

Cell growth was monitored using DNA concentration measurements with NanoDrop (ThermoScientific, NanoDrop 2000/2000c Spectrophotometer, λ = 260 nm) using the pre-made cell suspensions from *Section 2.5*. Protein expressions were analyzed using a Bradford Assay, where 3 mL of Bradford reagent was added to 100 µL sample volumes and absorbance measurements at 595 nm in a 96-well plate using the Tecan

Infinite M Plex Plate Reader. Absorbance levels were correlated to protein concentration using a calibration curve created from known BSA concentrations. Additionally, ATP levels were monitored using a lucerin-luciferase bioluminescence assay, where 30 µL of sample was added to 270 µL of reagent from an Invitrogen ATP Assay. In brief, the assay works based on luciferase's ability to produce light in the presence of ATP solely.

2.7 High-Resolution Liquid Chromatography-Mass Spectrometry (LC-MS)

Acid extractable organics (AEO) were first extracted from filtered photocatalytically and biologically treated samples using liquid-liquid extractions (LLEs). LLEs were performed by acidifying samples to pH 2 by adding H_2SO_4 in a dropwise manner. Samples were subsequently placed in a 500 mL separatory funnel, where 19 mL of DCM and 20 inversions were used in each extraction process. This was repeated thrice to collect a total of 57 mL of AEO samples, where the extraction efficiency was ~87% as measured by FTIR (Fig S.2) (PerkinElmer, Spectrum Two). Extracted AEO samples were subsequently blown down by gentle N_2 (g) sparging and were subsequently analyzed in negative ionization mode using UPLC-MS (Thermo Scientific Ultimate 3000 & Thermo Scientific Q Exactive) in BioZone at the University of Toronto (Toronto, Canada). A Thermo Scientific Hypersil Gold C18 column was used with a column temperature of 40˚C, autosampler temperature of 5˚C, injection volume of 10 µL, and a flow rate of 0.4 mL/min. Mass spectrometer settings were set at a 3.5 kV spray voltage; 320˚C capillary temperature, an m/z range of 100 – 1000; a resolution 17,500 with non-targeted data processing using Thermo Scientific Compound Discoverer 3.2 with Databases HMDB/KEGG/BioCyc, mzCloud.

3. Results and Discussion

3.1 Photocatalysis Enables Effective Mineralization of Naphthenic Acids with Improved Biokinetics

Synthetic OSPW was pre-treated under varying photocatalytic pre-treatment times (0 h - 2 d) prior to undergoing biological treatment. Soluble chemical oxygen demand (sCOD) levels were monitored in the biological treatment periodically to assess the pre-treatment time's impact on NA biodegradability and mineralization (Fig 1a). Fig 1a and Fig S.3 illustrate sCOD's exponential decrease with photocatalytic pre-treatment time, exhibiting a pseudo first-order constant of 0.025 h^{-1}. This agrees with previous BPC studies that demonstrated complete NA mineralization in OSPW with sufficient times [8–11]. The corresponding sCOD reduction is further resultant from the complete oxidation of lower molecular weight (MW) NAs, which preferentially degrade in TiO_2-based solar photocatalysis when treating technical grades [34]. The sCOD portion remaining, as demonstrated by O_o fractionation in S.4, is comprised of oxygenated NAs since BPCs preferentially and progressively supplements O-groups to NAs with complex moieties [11, 30, 35].

Nonetheless, Fig 1a illustrates no obvious improvement in biodegradability with short photocatalytic pre-treatment times (1 h – 8 h) when compared to the raw untreated control. These shorter pre-treatment times may have eliminated lower MW NAs without exhibiting sufficient times to supplement enough O_2-

groups into the remaining NA-fraction. Accordingly, longer pre-treatment times (≥ 1 d) with enhanced O_o (o > 2) fractionation (Fig S.4) demonstrated improved biodegradability, as sCOD levels diminished with biological treatment time. This improved biodegradability agrees with previous BPC studies which have shown the creation of oxy-NAs improves (biochemical oxygen demand) BOD:COD ratios (>0.3) and therefore NA biodegradability after sufficient treatment times [11, 35]. Thus, NAs require ≥1 d of pre-treatment to enhance biodegradability; a threshold requirement that has been observed for other NA pre-oxidative treatments (*e.g.,* ozonation, persulfate oxidation, and electro-oxidation) [23], [25]-[26], [32]-[33][23], [25]-[26], [32]-[33].

Fig 1b compares normalized sCOD levels for raw, 4 h, 1 d, and 2 d to standardize and therefore objectively compare the resulting biological treatments' performances. Raw and 4 h pre-conditions exhibited limited removal (~20-25%), coinciding with the lack of biodegradability. In contrast, 1 d ($p = 0.04$) and 2 d ($p = 0.001$) achieved ~52% and ~77% removal, respectively. Improvements in the 2 d pre-condition exceed that reported for ozonation under different biological treatment systems, such as IFAS (51%); suspended growth (53.8%); and persulfate oxidation with suspended microbial growth (30.8%) [17, 21, 37]. Table 2 summarizes the normalized sCOD removal rates and their p-values with respect to differences in the raw biologically treated samples, where p-values were calculated using a one-tailed student t-test.

Moreover, Table 2 compares the pseudo-first order kinetic constants calculated from Fig 1b's linear portions, yielding 0.012 d^{-1}, 0.023 d^{-1}, 0.064 d^{-1}, and 0.073 d^{-1} for the raw sample, 4 h, 1 d, and 2 d photocatalytic pre-treatments, respectively. The raw pseudo-constant agrees with previous reports, while the 1 d and 2 d preconditions exhibited a significant enhancement that superseded biokinetic-reports for electro-oxidation pre-treatments with graphite anodes (1.4 – 4.1-fold improvements), ozonation, and persulfate-oxidation (no improvements) [22], [25]-[26], [36][22],[22], [25]-[26], [36][26], [36]. Since bio-kinetics are not influenced by initial concentration, this enhancement corresponds to the improved O_o (o > 2) fractionation (Fig S.4) and biodegradability [38].

Finally, Fig 1c illustrates the long-term implications for biological treatment with an additional biosorption control. The bio-removal in the raw superseded previous reports with microbial suspensions (11.5 – 15.9%), removing ~20 – 30 mg/L (25 ± 9%) prior to levels rising, where a portion was removed via biosorption [15, 17, 19]. In contrast, 4 h and 1 d pre-treatments exhibited a large labile fraction until sCOD levels reached ~40 mg/L and 20 mg/L, respectively. The remaining sCOD portion exhibited recalcitrance since further removal was not apparent. Instead, an oscillation pattern was observed, providing evidence of cell lysis upon starvation and subsequent microbial uptake of lysate. Conversely, the 2 d pre-treatment time removed sCOD levels until the detection limit (3 mg/L) at 21 d, achieving complete mineralization at 33 d when considering the time required at the Athabasca Oil sands (Table 1). This demonstrates synergism between BPCs and microbes, since photocatalysis alone could not achieve complete mineralization at 7 d (168 h) of treatment which correlates to 42.2 d in the Athabasca Oil sands (Fig S.3, Table 1).

Moreover, the 4 h condition exhibited a lag time like that observed for electro-oxidation pre-treatments (10 d) and in which coincided with Fig 1 d' AEO-MS (acid-extractable fractions-mass spectrometry) trends

[19]. AEO-MS encompasses sCOD's hydrophobic organic-portions, as NA acid-extractability reduces upon their oxidation. Accordingly, AEO levels exponentially decayed as photocatalytic pre-treatment time progressed (Fig S.3), yielding a representative pseudo-first order constant of 0.13 h^{-1} [8, 9, 38]. Field studies using BPCs showed that at least 90% of AEO removal is required to eliminate OSPW total toxicity and recalcitrance [7]. Since the 4 h photocatalytic treatment could not reach 90% removal, a lag time occurred from these microbial metabolic impedances. In contrast, 1 d and 2 d photocatalytic times removed 96.8% and 99.1% AEO, respectively, while only the 2 d pre-condition allowed for near-complete (>99.9%) bio-removal of remaining AEO. These trends correlate with apparent sCOD recalcitrance, and 2 d pre-treatment's ability to remove ~100% of organics.

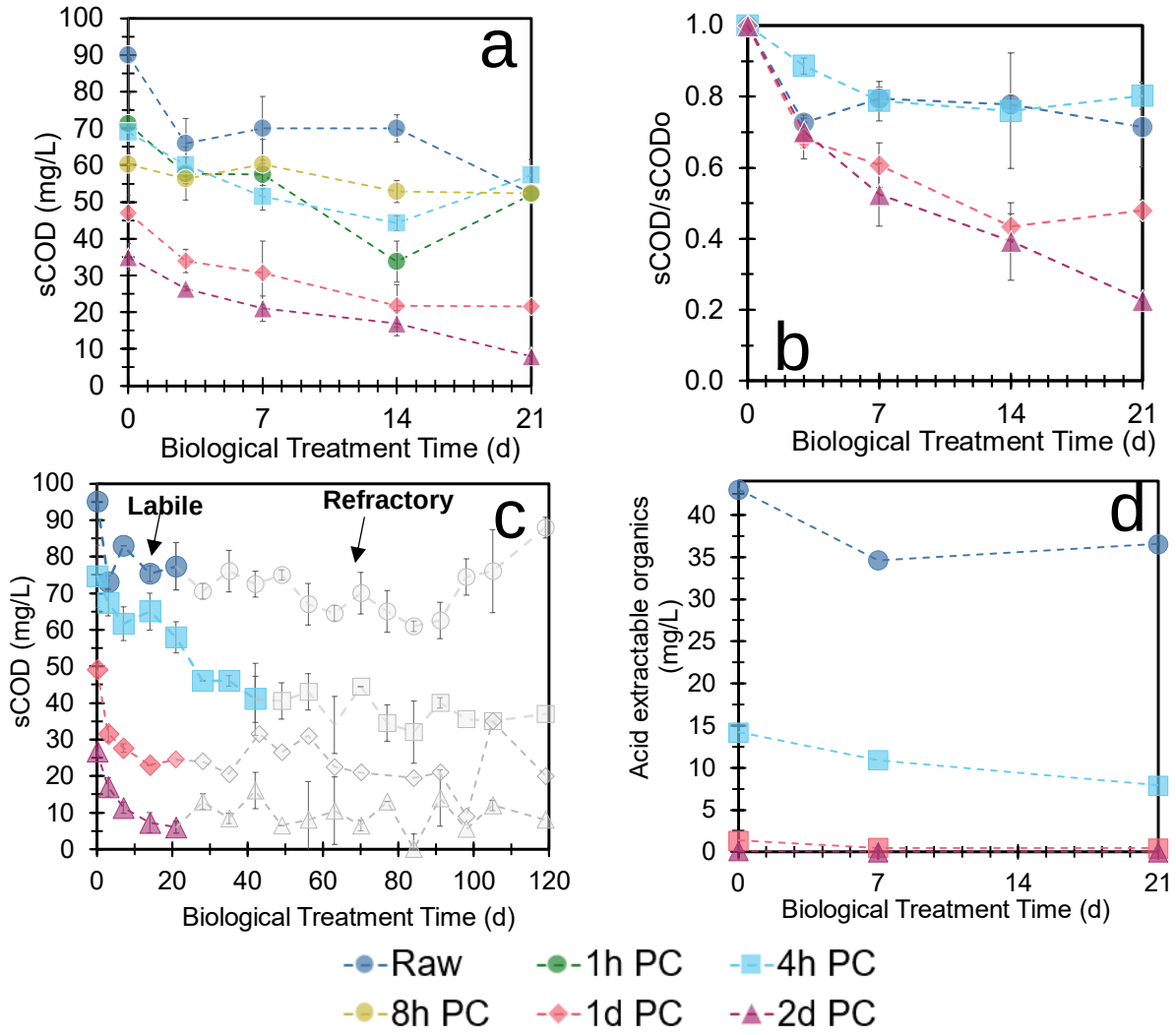

Fig 1. (a) Soluble chemical oxygen demand (sCOD, mg/L) removal as a function of biological treatment time (d) under different photocatalytic pre-treatment times (0h-2 d) **(b)** Relative sCOD removal as a function of biological treatment time (d) for raw, 4 h, 1 d, and 2 d (n = 3); **(c)** Long term sCOD (mg/L) removal as a function of biological treatment time (d) under different photocatalytic pre-treatment times (raw, 4 h, 1 d and 2 d) and for a biosorption control (*i.e.,* dead microbes) (n = 1); **(d)** Relative acid extractable organics removal as a function of biological treatment time (d) . Error bars represent standard deviation among trials.

Table 2. Summary of soluble chemical oxygen demand (sCOD) relative removal rates under different photocatalytic pre-treatment times at 21 days of biological treatment, their fitted pseudo-first order reaction rate constants, their respective p-values when compared against raw data, and their long-term bio- and total-removals observed after 120 days.

Photocatalytic Treatment Time (h)	Biological Relative sCOD Removal, $1 - {C}/{C_o}$ (t = 21 d)	Difference with no PC pre-treatment p-value	Biological Pseudo-First Order Rate Constants (d^{-1})	Difference with no PC pre-treatment p-value
0	0.23 ± 0.00	-	0.012 ± 0.003 (R^2 = 0.93)	-
4	0.20 ± 0.04	> 0.100	0.023 ± 0.015 (R^2 = 0.87)	> 0.10
24	0.52 ± 0.03	0.037	0.064 ± 0.009 (R^2 = 0.95)	0.037
48	0.77 ± 0.00	0.001	0.073 ± 0.008 (R^2 = 0.91)	0.023

3.2 Photocatalysis Improves Microbial Growth, Protein Production, and ATP Production

Microbial DNA mass (Fig 2a), protein mass (Fig 2b), and metabolic activity (Fig 2c) per sCOD levels were monitored periodically to understand the microbial response under different photocatalytic pre-treatment times. Each parameter was normalized to sCOD levels to compare microbial functionality under different organic concentrations. Understanding microbial community profiles and shifts were deemed out of scope for this study and will be assessed in future on real OSPW. As shown, the untreated raw sample's DNA and protein profiles indicate a lag time of 3d, which corresponds to the lack of labile organics observed in Fig 1. Lag times are well-reported for the biological treatment of OSPW due to untreated NAs' steric hindrances (*e.g.,* branching, rings) that block NA-metabolic routes [12, 19, 37, 39]. Additionally, a stationary phase that maintained normalized DNA and protein levels at ~0.25 ng-DNA/mg-sCOD and ~7.10 mg-protein/mg-sCOD, respectively, prevailed after a log phase between 3 – 7 d.

Lag phases were eliminated with photocatalytic pre-treatments since photocatalysis preferentially oxidizes NAs with greater structural complexity, thereby removing steric hindrances and creating labile organic forms for microbial metabolism [11]. This phenomenon has been seen for ozonation pre-treatments [36, 37]. Additionally, the photocatalytic pre-treatment DNA profiles exhibited stationary phases followed by an additional log growth phase which correlated with their respective sCOD removals. This is indicative that there are either: (1) adaptation periods or (2) the microbes are intermittently activating remaining organics to labile forms (*i.e.,* oxygenating). On the other hand, protein levels followed a saturation curve, where a higher maximum normalized protein level was reached with higher photocatalytic pre-treatment times. The profile differences are likely from protein levels capturing the upregulation of enzyme production upon photocatalytic pre-treatments; a phenomenon that's been observed for methyl red biological treatments with ZnO-based photocatalytic pre-treatments [24].

Microbial growth measured by normalized DNA and protein levels were positively correlated to photocatalytic pre-treatment times, exhibiting 4-, 10-, and 23-fold increases for 4 h, 1 d, and 2 d, respectively for DNA levels and 2-, 6-, and 25-folds for 4 h, 1 d, and 2 d respectively for protein levels. Statistically significant ($p < 0.04$) first order and second-order relationships were found for normalized DNA levels (Fig S.5, R^2 = 0.98) and proteins levels (Fig S.7, R^2 = 0.95), respectively, when assessed as a function of

photocatalytic pre-treatment time. These correlations indicate that increasing NA hydrophilicity with increased photocatalytic pre-treatment times create more labile organics for microbial metabolism. These relationships further coincide with persulfate and ozonation pre-treatment studies that found greater gene copies upon NA oxidation, that was upwards of 100-folds using biofilms [15, 17, 39]. Additionally, like ozonation pre-treatment studies, NA pre-oxidation using photocatalysis enabled greater normalized microbial growth rates [36, 37].

Moreover, the untreated raw samples exhibited negligible ATP levels that did not surpass 35 ng-DNA/mg-sCOD. The 4 h and 1 d conditions exhibited a spike in metabolic activities at 3 d with subsequent diminishing levels as biological treatment persisted. These peaks agree with their labile organic fractions in Fig 1, where once these diminished there was an upregulation of ATP-requirements for enzyme production, which coincides with the intermittent growth adaptation periods. In contrast, the 2 d pre-condition's ATP levels increased and were sustained for 7 d until the organics diminished (Fig 1), thereby demonstrating no required adaptation periods to metabolize remaining organics. Overall, these metabolic improvements coincide with a mild ozonation and a ZnO-based photocatalytic pre-treatment study which demonstrated an upregulation of microbial metabolism when treating NAs and methyl red, respectively [18], [25][18], [25].

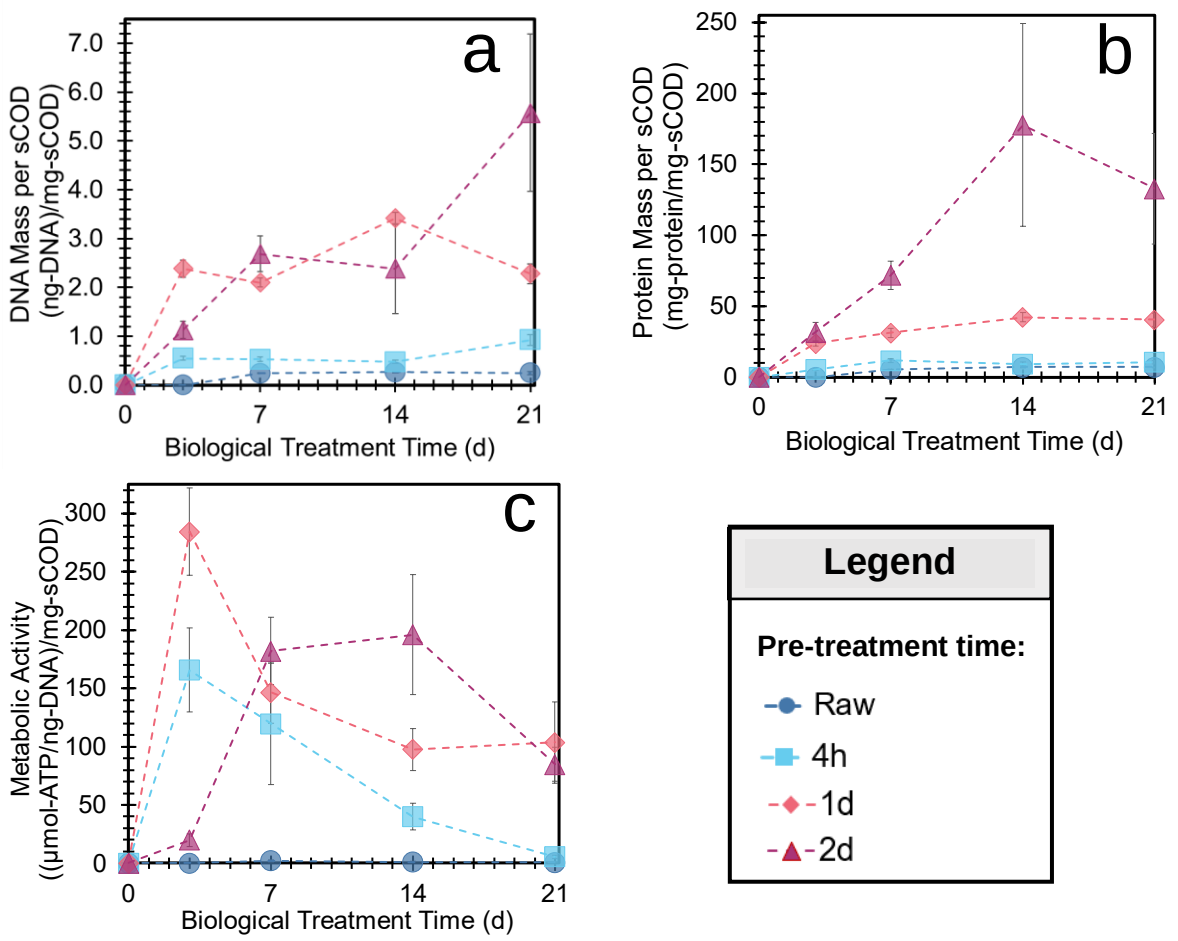

Fig 2. (a) DNA yield per soluble chemical oxygen demand (sCOD) (ng-DNA/mg-sCOD) as a function of biological treatment time (d) under different photocatalytic pre-treatment times; **(b)** Protein yield per sCOD (mg-protein/mg-sCOD) as a function of biological treatment time (d) under different photocatalytic pre-treatment times; **(c)** Metabolic activity (µmol-ATP/mg-sCOD) as a function of biological treatment time (d) under different photocatalytic pre-treatment times. Error bars represent standard deviation among two trials (n = 2).

3.3 Photocatalytic and Microbial Transformation of Naphthenic Acids Under Different Pre-Treatments

LC-MS analyses were conducted on the acid-extractable organics (AEO) in duplicates under negative ionization mode to understand NA's photo- and bio-conversions throughout treatment and how their dynamic chemical speciation may have affected microbial growth, protein production, and metabolism. Fig 3 a-c illustrate NAs' positive shift in average molecular weight (MW, g/mol), oxygen to carbon ratio (O/C) and double bond equivalence (DBE) as a function of photocatalytic pre-treatment time (h), respectively. All three relationships demonstrated strong positive correlations ($R^2 > 0.80$) that were statistically significant using two-tailed t-tests ($p < 0.01$). Thus, photocatalysis enriched OSPW with high MW NAs with greater oxygenation levels upon treatment which agrees with another TiO_2-based solar photocatalytic pre-treatment study on synthetic NAs [38]. The progressive shift towards higher MW may be from (1) the oxidation of

lower MW NAs to CO_2 and/or (2) photocatalytic conversion of O_2-NAs to oxy-NAs. The latter is supported by their O_o ($o \geq 2$) fractionation (Fig S.4) and the O/C trend that is well reported for BPC treatments [35]. Nonetheless, the enrichment of higher MW NAs without sufficient O_2-insertion would explain the recalcitrance at lower pre-treatment times (<1 d). Furthermore, the positive shift in DBE contradicts BPC studies that demonstrated preferential removal with higher DBEs [35]. Since synthetic NAs contain more simplistic NAs with lower oxygenation, this could be indicative of (1) the rapid removal of more simplistic NAs with pi-bonds and/or (2) the addition of O_2-groups without mineralization which correlates with our O/C trends.

The biotransformation of NAs' MW, O/C, and DBE shifts at 0 d, 7 d, and 21 d of biological treatment were profiled for raw (Fig 3d; 3i; 3n), 4 h (Fig 3e; 3j; 3o), 1 d (Fig 3f; 3k; 3p), and 2 d (Fig 3g; 3l; 3q) pre-treatments, respectively along with their average values as a function of biological treatment time (Fig 3h; 3m; 3r). Microbes in the untreated raw removed a limited number of NAs in the lower MW realm (< 300 g/mol), maintaining the same average MW as bio-time persisted. This coincides with the raw water's low O/C and recalcitrance (Fig 1). The 4 h photocatalytic pre-treatment removed >50% of NAs and enabled their biological reduction at ~180-200 g/mol with the simultaneous formation of a 160 g/mol peak. Simultaneously, microbes increased O/C upon biological treatment, creating peaks around 0.3. This is indicative of microbial biotransformation of higher MW NAs to lower MW NAs with higher oxygenation levels, thereby yielding greater labile fractions (Fig 1); nonetheless, no significant shifts in average values were observed.

1 d and 2 d pre-treatment times removed >90% of NAs and created an upward shift in MW. The 1 d pre-treatment created a larger MW range (200 – 400 g/mol), where the lower portion (< 250 g/mol) was eliminated in the 2 d condition. Microbial biotransformation of higher MW NAs to lower MW NAs were apparent in both cases but was enhanced in the 2 d condition as indicated by its significant average MW reduction as bio-time persisted. Additionally, these removals correlated with higher carbon numbers (Fig S.8) and DBEs (>3), thereby indicating NA MW increases is imparted by NA carboxylation since higher DBEs from alkyl branching and rings would have increased recalcitrance. These trends agree with ozonation and electro-oxidation pre-treatment studies which found biotransformations of higher carbon numbers to lower carbon numbers [16, 19, 30].

Furthermore, the sporadic O/C and DBE fluctuations along with the creation of lower MW NA peaks for most pre-treated samples, are indicative of microbial O_2-insertion (*e.g.,* monooxygenase) and NA decarboxylation via β-oxidation [13], [25]. This agrees with electro-oxidation studies that have demonstrated microbial O_2-insertion with aerobic post biological treatments [19, 30]. Nonetheless, O/C decreased upon biological treatment in the 2 d pre-condition, owing to its enrichment of oxy-NAs that negates microbial O_2-insertion requirements to initiate metabolism.

Fig S.9 correlates these photo-transformations of O/C, MW, and DBE to normalized DNA-, protein, and ATP levels. Normalized DNA levels were positively correlated to DBE ($p = 0.05$), thereby providing further evidence NA DBE increased from oxygenation that activated organics for metabolic uptake. The

lack of correlation for O/C and MW stem from the sporadic changes observed upon biotransformation, as this contradicts microbial profiles in Fig 2. Similarly, no trends were observed for ATP levels, which stems from the ATP's peaked profiles. Nonetheless, NA bio-removal increased upon increasing pre-treatments as indicated by the total intensity reduction. Such improvements have been seen for ozonation pre-treatments that demonstrated greater biodegradability with higher NA oxidation states [16–20, 30, 39, 40]. However, dosage considerations can be negated since photocatalytic oxidants do not leave remaining oxidants in the water, unlike ozone

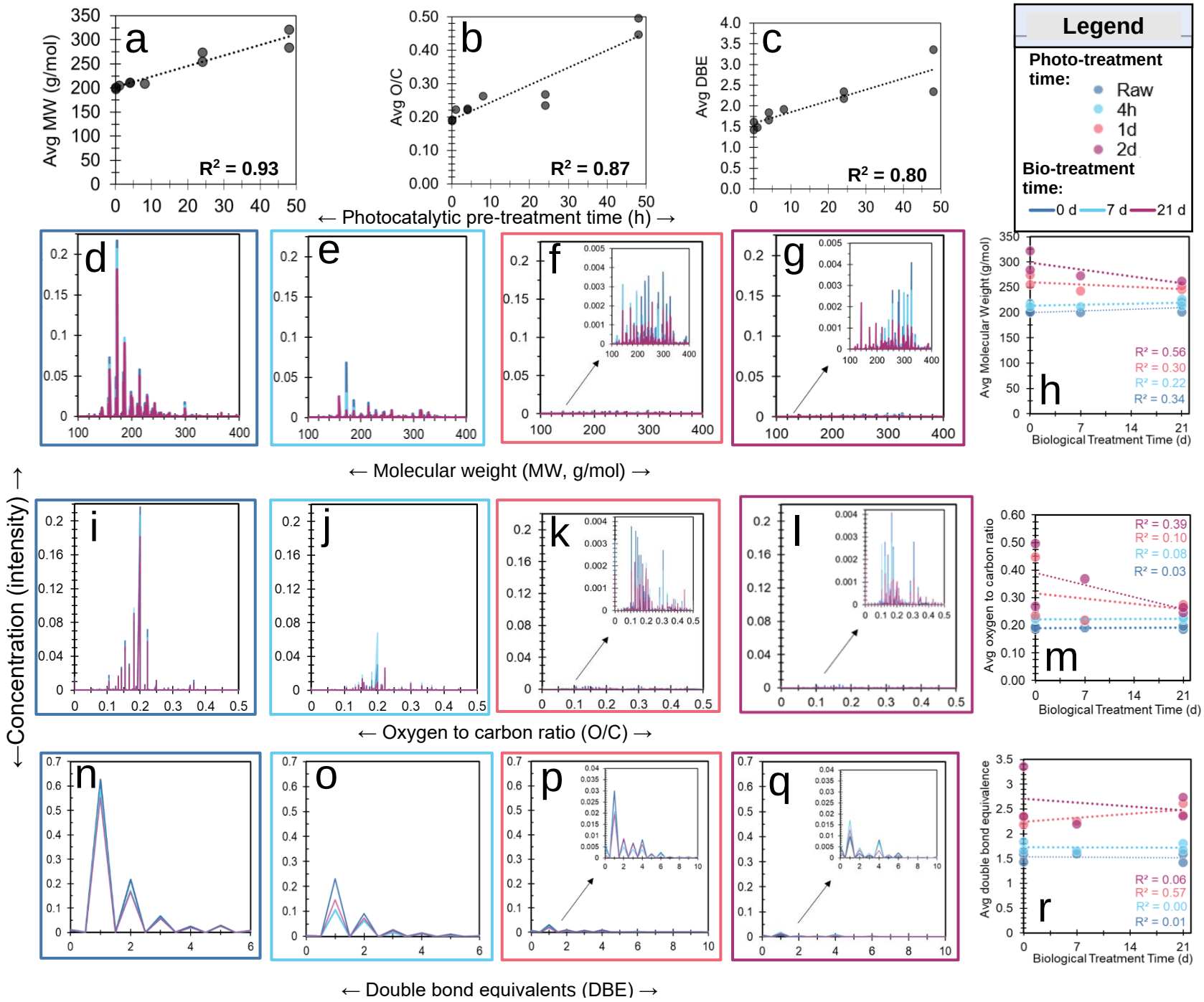

Fig 3. a-c average MW (g/mol), O/C, and DBE as a function of photocatalytic pre-treatment time (h), respectively. **d-g** illustrate MW (g/mol) **i-l** O/C **n-q** DBE concentration spectra for raw, 4 h, 1 d, and 2 d pre-treatment times for 0 d (blue); 7 d (cyan) and 21 d (purple), respectively. **h, m and r** illustrate average MW (g/mol), O/C and DBE for raw, 4 h, 1 d, and 2 d pre-treatment times, respectively

3.4 Photocatalysis Removes Microbial Inhibition with Sufficient Pre-Treatment Times

NAs are the contaminant of concern for OSPW due in part to their surfactant properties that enable them to penetrate cellular membranes, disrupt their properties and, in turn, cause cellular death [6, 36]. Their toxicity is proportional to their concentration, polarity, carbon number, cyclicity, molecular weight, and alkyl branching, where the addition of carboxylic acid functional groups via photocatalysis can reduce individual NA's toxicity [1]. BPCs have already been shown capable of eliminating toxicity in *A. fischeri,* a model organism in Microtox Assays, by preferentially targeting concerning NA functional groups (*e.g.,* O_2^{2-}) [35]. Herein, our goal was to understand toxicity at the microscopic level and BPC treatments impact on microbial functionality. Accordingly, inhibition tests were conducted by supplementing acetate in raw and photocatalytically treated OSPW to assess microbes' ability to uptake a labile organic in the presence of non-treated and treated NAs.

Fig 4 depicts the resulting (a) sCOD and (b) OD measurements for each condition. If the pre-treatments removed toxicity at the microscopic level than the metabolic uptake of acetate and microbial growth should resemble the control without NAs. Without photocatalytic pre-treatment, sCOD was reduced from ~900 mg/L to ~750 mg/L, while OD levels were maintained at 0.04. This coincides with the limited growth and sCOD/AEO removal observed for the raw water in Fig 2 and 1, respectively. The 4 h photocatalytic pre-treatment resulted in a further decrease in sCOD from ~900 mg/L to ~550 mg/L but was ultimately inhibited since it did not reach the same degradation rates as the control. Its inhibition coincides with its remaining AEO fraction and sCOD profiles after >100 d of biological treatment (Fig 1). It further compliments a TiO_2-based solar photocatalytic study which showed >5 h was required to eliminate toxicity in D. *magna* and P. *promelas* [34]. Interestingly, microbial growth rates were not limited. Although there was an apparent lag phase for ~5 d, the 4 h condition exhibited a growth rate that superseded the control, reaching OD levels of ~0.13 (1.5x greater). It is unclear the reasons for this growth trend from this study, but it may be attributed to the presence of steroid-like NAs which have been identified as growth promoters among certain bacterial species [41, 42].

Alternatively, 1 d and 2 d pre-treatment conditions exhibited sCOD removal rates and extents that resembled the control without NAs, attaining sCOD levels from ~850 to ~150 mg/L by day 14. Thus, toxicity was eliminated in both conditions at the microscopic level which coincides with a BPC study that demonstrated chronic toxicity could be fully eliminated only with >90% NA degradation [7]. However, only the 2 d pre-treatment resembled similar growth rates to the control as the 1 d condition exhibited growth rates that resembled the 4 h pre-treatment condition. This may be from the presence of steroid NAs since 1 d did not eliminate AEO.

Overall, the toxicity reduction observed supersede ozonation which experienced minimal detoxification upon mild ozonation, and even experienced greater toxicity in a 73% ozone degraded Merichem NA sample [39]. Likewise, another ozonation study demonstrated a 34.2% and 40.9% level of inhibition after the elimination of 90% of NAs with 30 mg/L and 80 mg/L dosages, respectively [28]. The creation of toxic by-products is non-evident from the present study, which demonstrates continual detoxification upon

increasing photocatalytic pre-treatment times. Furthermore, the level of inhibition reduction surpassed electro- and persulfate-oxidation, thereby rendering photocatalysis as an environmental benign pre-treatment for in-situ biological treatments [18, 19].

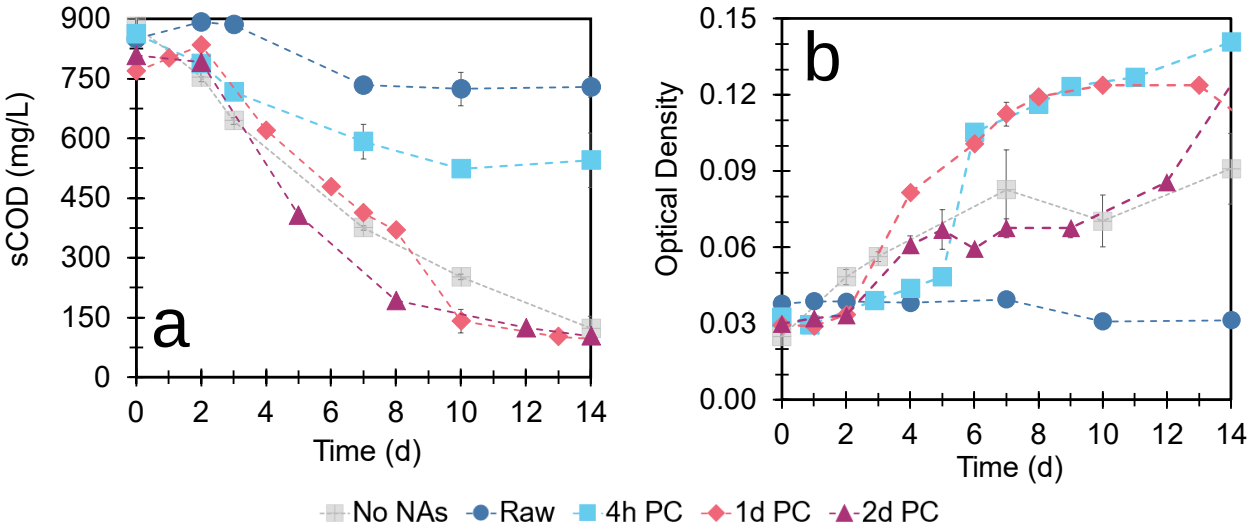

Fig 3. Microbial inhibition test results for **(a)** soluble chemical oxygen demand (sCOD, mg/L) and **(b)** optical density as a function of time for different photocatalytic pre-treatment times, raw and a control without naphthenic acids (NA). Error bars represent standard deviation among sCOD measurements (n = 2).

4. Conclusions

This study explored BPCs efficacy as a pre-treatment for the biological degradation of NAs in synthetic OSPW. Our findings demonstrate that increasing photocatalytic pre-treatment time increased NA biodegradability, where ≥1 d pre-treatment times exhibited statistically significant enhancements in relative organics (sCOD and AEO) bio-removal and bio-kinetics. The 2 d bio-kinetics enhancement created synergism, demonstrating mineralization rates that could not be accomplished by BPCs alone and therefore rendering the pre-treatment time optimal to reduce both treatment time and dosage requirements for OSPW remediation. Enhancement in performance seen for 2 d was correlated to 23-fold increases in normalized DNA yields; sustained ATP productions; and elimination of inhibition. LC-MS analyses provided evidence that the 2 d condition enriched OSPW with oxy-NAs that eliminated microbial O_2-insertion requirements to initiate microbial metabolism. Overall, our study demonstrates BPCs' ability to be employed as a fully passive system OSPW under mild conditions that will enable the full mineralization of NAs in a post *in-situ* biological treatment. Overall, BPCs offer an environmental-benign treatment due to their ability to be recycled without the addition of oxidative chemicals and the potential of toxic by-product production (*e.g.,* ozone) [10]. Nonetheless, future studies should assess the efficacy with real OSPW and how these systems work with other microorganism (*e.g.,* algae and anaerobes).

Author Contributions

Cassandra Chidiac: Methodology, Validation, Formal analysis, Investigation, Visualization, Writing – original draft, Writing – review & editing. Tim Leshuk: Conceptualization, Methodology, Supervision, Writing – review & editing. Frank Gu: Conceptualization, Methodology, Supervision, Writing – review & editing.

Acknowledgements

Liquid chromatography mass spectrometry analyses were conducted in BioZone at the University of Toronto by Robert Flick. The authors would further like to acknowledge Endang Susilawati for her guidance and training on required instruments.

Funding Sources

This work is supported by Natural Sciences and Engineering Research Council (NSERC) Postgraduate Scholarships-Doctoral (PGS-D) program.

5. References

1. Wu C, de Visscher A, Gates ID (2019) On naphthenic acids removal from crude oil and oil sands process-affected water. Fuel 253:1229–1246. https://doi.org/10.1016/J.FUEL.2019.05.091
2. Kannel PR, Gan TY (2012) Naphthenic acids degradation and toxicity mitigation in tailings wastewater systems and aquatic environments: A review. J Environ Sci Health A Tox Hazard Subst Environ Eng 47:1–21. https://doi.org/10.1080/10934529.2012.629574
3. Milestone CB, Sun C, Martin JW, et al (2020) Non-target profiling of bitumen-influenced waters for the identification of tracers unique to oil sands processed-affected water (OSPW) in the Athabasca watershed of Alberta, Canada Funding information Canada-Alberta Oil Sands Monitoring Program; Environment and Climate Change Canada. https://doi.org/10.1002/rcm.8984
4. Madison BN, Reynolds J, Halliwell L, et al (2020) Can the toxicity of naphthenic acids in oil sands process-affected water be mitigated by a green photocatalytic method? Facets 5:474–487. https://doi.org/10.1139/FACETS-2019-0053
5. Huang R, Chen Y, Meshref MNA, et al (2018) Characterization and determination of naphthenic acids species in oil sands process-affected water and groundwater from oil sands development area of Alberta, Canada. Water Res 128:129–137. https://doi.org/10.1016/j.watres.2017.10.003
6. Quinlan PJ, Tam KC (2015) Water treatment technologies for the remediation of naphthenic acids in oil sands process-affected water. Chemical Engineering Journal 279:696–714. https://doi.org/10.1016/j.cej.2015.05.062
7. Madison BN, Reynolds J, Halliwell L, et al (2020) Can the toxicity of naphthenic acids in oil sands process-affected water be mitigated by a green photocatalytic method? Facets 5:474–487. https://doi.org/10.1139/FACETS-2019-0053/SUPPL_FILE/FACETS-2019-0053_SUPPLEMENT1.DOCX
8. Leshuk T, Peru KM, de Oliveira Livera D, et al (2018) Petroleomic analysis of the treatment of naphthenic organics in oil sands process-affected water with buoyant photocatalysts. Water Res 141:297–306. https://doi.org/10.1016/j.watres.2018.05.011
9. Leshuk T, de Oliveira Livera D, Peru KM, et al (2016) Photocatalytic degradation kinetics of naphthenic acids in oil sands process-affected water: Multifactorial determination of significant factors. Chemosphere 165:10–17. https://doi.org/10.1016/j.chemosphere.2016.08.115
10. Leshuk T, Krishnakumar H, Livera D de O, Gu F (2018) Floating photocatalysts for passive solar degradation of naphthenic acids in oil sands process-affected water. Water (Switzerland) 10:. https://doi.org/10.3390/w10020202
11. de Oliveira Livera D, Leshuk T, Peru KM, et al (2018) Structure-reactivity relationship of naphthenic acids in the photocatalytic degradation process. Chemosphere 200:180–190. https://doi.org/10.1016/j.chemosphere.2018.02.049

12. Han X, Scott AC, Fedorak PM, et al (2008) Influence of molecular structure on the biodegradability of naphthenic acids. Environ Sci Technol 42:1290–1295. https://doi.org/10.1021/es702220c
13. Kumar G, Prasad JS, Suman A, Pandey G (2019) Bioremediation of petroleum hydrocarbon-polluted soil using microbial enzymes. Elsevier Inc.
14. Misiti TM, Tezel U, Tandukar M, Pavlostathis SG (2013) Aerobic biotransformation potential of a commercial mixture of naphthenic acids. Water Res 47:5520–5534. https://doi.org/10.1016/j.watres.2013.06.032
15. Hwang G, Dong T, Islam MS, et al (2013) The impacts of ozonation on oil sands process-affected water biodegradability and biofilm formation characteristics in bioreactors. Bioresour Technol 130:269–277. https://doi.org/10.1016/j.biortech.2012.12.005
16. Zhang L, Zhang Y, Gamal El-Din M (2018) Degradation of recalcitrant naphthenic acids from raw and ozonated oil sands process-affected waters by a semi-passive biofiltration process. Water Res 133:310–318. https://doi.org/10.1016/J.WATRES.2018.01.001
17. Zhang L, Zhang Y, Gamal El-Din M (2019) Integrated mild ozonation with biofiltration can effectively enhance the removal of naphthenic acids from hydrocarbon-contaminated water. Science of The Total Environment 678:197–206. https://doi.org/10.1016/J.SCITOTENV.2019.04.302
18. Ganiyu SO, Arslan M, Gamal El-Din M (2022) Combined solar activated sulfate radical-based advanced oxidation processes (SR-AOPs) and biofiltration for the remediation of dissolved organics in oil sands produced water. Chemical Engineering Journal 433:134579. https://doi.org/10.1016/J.CEJ.2022.134579
19. Abdalrhman AS, Zhang Y, Gamal El-Din M (2019) Electro-oxidation by graphite anode for naphthenic acids degradation, biodegradability enhancement and toxicity reduction. Science of the Total Environment 671:270–279. https://doi.org/10.1016/J.SCITOTENV.2019.03.262
20. Zhang Y, Xue J, Liu Y, Gamal El-Din M (2016) Treatment of oil sands process-affected water using membrane bioreactor coupled with ozonation: A comparative study. Chemical Engineering Journal 302:485–497. https://doi.org/10.1016/J.CEJ.2016.05.082
21. Huang C, Shi Y, Gamal El-Din M, Liu Y (2015) Treatment of oil sands process-affected water (OSPW) using ozonation combined with integrated fixed-film activated sludge (IFAS). Water Res 85:167–176. https://doi.org/10.1016/J.WATRES.2015.08.019
22. Yu M, Wang J, Tang L, et al (2020) Intimate coupling of photocatalysis and biodegradation for wastewater treatment: Mechanisms, recent advances and environmental applications. Water Res 175:115673. https://doi.org/10.1016/j.watres.2020.115673
23. Zhang C, Li Y, Shen H, Shuai D (2021) Simultaneous coupling of photocatalytic and biological processes: A promising synergistic alternative for enhancing decontamination of recalcitrant compounds in water. Chemical Engineering Journal 403:. https://doi.org/10.1016/j.cej.2020.126365

24. Waghmode TR, Kurade MB, Sapkal RT, et al (2019) Sequential photocatalysis and biological treatment for the enhanced degradation of the persistent azo dye methyl red. J Hazard Mater 371:115–122. https://doi.org/10.1016/j.jhazmat.2019.03.004

25. Bhatia V, Dhir A, Ray AK (2018) Integration of photocatalytic and biological processes for treatment of pharmaceutical effluent. J Photochem Photobiol A Chem 364:322–327. https://doi.org/10.1016/j.jphotochem.2018.06.027

26. Yahiat S, Fourcade F, Brosillon S, Amrane A (2011) Removal of antibiotics by an integrated process coupling photocatalysis and biological treatment - Case of tetracycline and tylosin. Int Biodeterior Biodegradation 65:997–1003. https://doi.org/10.1016/j.ibiod.2011.07.009

27. Moo-Young M, Anderson WA, Zhang Z (2002) Photocatalytic pretreatment of contaminated groundwater for biological nitrification enhancement. Journal of Chemical Technology and Biotechnology 77:190–194. https://doi.org/10.1002/jctb.547

28. Wang N, Chelme-Ayala P, Perez-Estrada L, et al (2013) Impact of ozonation on naphthenic acids speciation and toxicity of oil sands process-affected water to vibrio fischeri and mammalian immune system. Environ Sci Technol 47:6518–6526. https://doi.org/10.1021/ES4008195/SUPPL_FILE/ES4008195_SI_001.PDF

29. Balaberda AL, Ulrich AC (2021) Persulfate oxidation coupled with biodegradation by pseudomonas Fluorescens enhances naphthenic acid remediation and toxicity reduction. Microorganisms 9:. https://doi.org/10.3390/MICROORGANISMS9071502

30. Abdalrhman AS, Zhang Y, Arslan M, Gamal El-Din M (2020) Low-current electro-oxidation enhanced the biodegradation of the recalcitrant naphthenic acids in oil sands process water. J Hazard Mater 398:122807. https://doi.org/10.1016/J.JHAZMAT.2020.122807

31. Damasceno FC, Gruber LDA, Geller AM, et al (2014) Characterization of naphthenic acids using mass spectroscopy and chromatographic techniques: Study of technical mixtures. Analytical Methods 6:807–816. https://doi.org/10.1039/c3ay40851e

32. Leshuk T, Wong T, Linley S, et al (2016) Solar photocatalytic degradation of naphthenic acids in oil sands process-affected water. Chemosphere 144:1854–1861. https://doi.org/10.1016/j.chemosphere.2015.10.073

33. Metcalf E (2004) Wastewater Engineering Treatment and Reuse (4th edition) (2004) | Akhid Maulana - Academia.edu, 4th ed

34. Mishra S, Meda V, Dalai AK, et al (2010) Photocatalysis of Naphthenic Acids in Water. J Water Resource and Protection 2:644–650. https://doi.org/10.4236/jwarp.2010.27074

35. Leshuk T, Wong T, Linley S, et al (2016) Solar photocatalytic degradation of naphthenic acids in oil sands process-affected water. Chemosphere 144:1854–1861. https://doi.org/10.1016/J.CHEMOSPHERE.2015.10.073

36. Dong T, Zhang Y, Islam MS, et al (2015) The impact of various ozone pretreatment doses on the performance of endogenous microbial communities for the remediation of oil sands process-affected water. Int Biodeterior Biodegradation 100:17–28. https://doi.org/10.1016/J.IBIOD.2015.01.014

37. Meshref MNA, Chelme-Ayala P, Gamal El-Din M (2017) Fate and abundance of classical and heteroatomic naphthenic acid species after advanced oxidation processes: Insights and indicators of transformation and degradation. Water Res 125:62–71. https://doi.org/10.1016/J.WATRES.2017.08.007

38. Sabyasachi M, Venkatesh M, Ajay K. D, et al (2010) Photocatalysis of Naphthenic Acids in Water. J Water Resour Prot 2010:644–650. https://doi.org/10.4236/JWARP.2010.27074

39. Ozonation of Oil Sands Process-Affected Water Accelerates Microbial Bioremediation. https://doi.org/10.1021/es101556z

40. Yanyan JX, Yang Z, Mohamed L, El-Din G Treatment of raw and ozonated oil sands process-affected water under decoupled denitrifying anoxic and nitrifying aerobic conditions: a comparative study. Biodegradation 27:. https://doi.org/10.1007/s10532-016-9770-9

41. Buetow DE, Levedahl BH RESPONSES OF MICROORGANISMS TO STEROLS AND STEROIDS1.2

42. Rowland SJ, West CE, Jones D, et al (2011) Steroidal Aromatic “Naphthenic Acids” in Oil Sands Process-Affected Water: Structural Comparisons with Environmental Estrogens. Environ Sci Technol 45:9806–9815. https://doi.org/10.1021/es202606d